JOURNAL OF SYNCHROTRON RADIATION

ISSN 1600-5775

Received 9 May 2019
Accepted 24 June 2019

Edited by M. Yamamoto, RIKEN SPring-8 Center, Japan

Keywords: serial crystallography; sample delivery; syringe pumps; viscous media; lipidic cubic phase; polyacrylamide.

PDB references: room-temperature structure of lysozyme delivered in LCP by serial millisecond crystallography, 6jxp; room-temperature structure of lysozyme delivered in polyacrylamide by serial millisecond crystallography, 6jxq

Supporting information: this article has supporting information at journals.iucr.org/s

Sample delivery using viscous media, a syringe and a syringe pump for serial crystallography

Suk-Youl Park[a]* and Ki Hyun Nam[b,c]*

[a]Pohang Accelerator Laboratory, POSTECH, Pohang, Gyeongbuk 37673, Republic of Korea, [b]Division of Biotechnology, Korea University, Seoul 02841, Republic of Korea, and [c]Institute of Life Science and Natural Resources, Korea University, Seoul 02841, Republic of Korea. *Correspondence e-mail: navypsy@postech.ac.kr, structures@korea.ac.kr

Sample delivery using injectors is widely used in serial crystallography (SX) and has significantly contributed to the determination of crystal structures at room temperature. However, sophisticated injector nozzle fabrication methods and sample delivery operations have made it difficult for ordinary users to access the SX research. Herein, a simple and easily accessible sample delivery method for SX experiments is introduced, that uses a viscous medium, commercially available syringe and syringe pump. The syringe containing the lysozyme crystals embedded in lipidic cubic phase (LCP) or polyacrylamide (PAM) delivery media was connected to a needle having an inner diameter of 168 µm, after which it was installed on a syringe pump. By driving the syringe pump, the syringe plunger was pushed and the crystal sample was delivered to the X-ray beam position in a stable manner. Using this system, the room-temperature crystal structures of lysozyme embedded in LCP and PAM at 1.56 Å and 1.75 Å, respectively, were determined. This straightforward syringe pump-based sample delivery system can be utilized in SX.

1. Introduction

Serial crystallography (SX) using an X-ray free-electron laser (XFEL) or synchrotron radiation allows the determination of room-temperature crystal structures without radiation damage or at low-dose data collection, respectively (Chapman *et al.*, 2014; Nogly *et al.*, 2015; Weinert *et al.*, 2017; Kim *et al.*, 2018). These techniques provide information regarding conformational flexibility of the macromolecule at room temperature and allow time-resolved studies with time resolutions ranging from femtoseconds to seconds or longer (Weinert *et al.*, 2017; Schulz *et al.*, 2018). In SX experiments, an important aspect is the delivery of the crystal samples stably and continuously to the X-ray beam position (Grünbein & Kovacs, 2019). The sample delivery method using an injector with a viscous medium dramatically reduced the sample consumption when compared with other injector-based sample delivery methods (Nam, 2019). However, injectors that deliver common viscous media require skilled operation using an elaborately manufactured nozzle (Weierstall *et al.*, 2014; Bohne *et al.*, 2019). Conversely, a simple method of delivering viscous media containing crystals from a syringe by stepper-motor driving has also been reported (Sugahara *et al.*, 2015). However, a user-friendly sample delivery system is still required for the selection of appropriate delivery media and injection tests in the pre-experiment or for user-driven sample delivery during beam time.

Herein, we introduce straightforward sample delivery methods using commercially available syringes and syringe

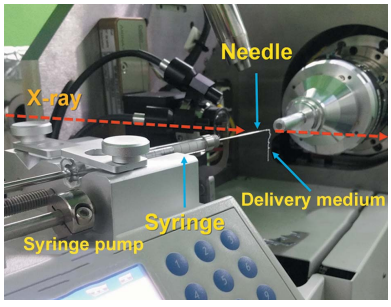

pumps which can easily be accessed for the SX experiment. Using this system, the lysozyme crystals embedded in the lipidic cubic phase (LCP) and polyacrylamide (PAM) were delivered and the room-temperature crystal structures were determined at 1.56 Å and 1.76 Å, respectively. Our approach will be useful for screening suitable delivery media and for data collection in the SX experiment.

2. Experimental procedure

Serial millisecond crystallography (SMX) using a syringe pump was performed on the microfocusing beamline 11C at Pohang Light Source II (Park *et al.*, 2017). The X-ray beam size focused by a Kirkpatrick–Baez mirror was 4.1 µm (vertical) × 8.5 µm (horizontal) at the sample position. The photon flux and beam energy were 1.3×10^{12} photons s^{-1} and 12.659 keV, respectively. The crystallization of lysozyme from chicken egg white was performed using a previously reported procedure (Lee *et al.*, 2019). The lysozyme crystals were embedded in the sample delivery medium (LCP or PAM) using mechanical mixing in a dual-syringe setup. A 100 µl syringe (Hamilton, 81065-1710RNR) containing the crystals embedded in the delivery medium was mounted on a Fusion Touch 100 syringe pump (CHEMYX). The syringe needle with an inner diameter of 168 µm was monitored by an on-axis video microscope installed in the MD2-S goniometer (Arinax) in the beamline hutch [Fig. 1(*a*)]. To align the syringe needle on the syringe pump to the X-ray beam path, a manual stage was installed under the syringe pump stand to make fine adjustments in the *x*, *y* and *z* directions. Due to the interference of the beamline equipment and the syringe pump, the syringes and needles were installed horizontally [Fig. 1(*a*)]. Considering the stream direction of the delivery medium from the syringe needle, the needle end of the syringe was aligned at approximately 100 µm from the beam path, 45° diagonally upward using manual stages [Figs. 1(*b*) and 1(*c*)]. By driving the syringe pump, LCP- and PAM-containing crystals were extruded from the syringe needle to the X-ray position at flow rates of 100 nl min^{-1} and 200 nl min^{-1}, respectively [Figs. 1(*b*) and 1(*c*)]. During data collection, all images were exposed for 100 ms. The temperature and humidity inside the hutch were 25 ± 0.4°C and 20%, respectively. Images were pre-filtered using *Cheetah* (Barty *et al.*, 2014) and processed using *CrystFEL* (White *et al.*, 2016). Molecule replacement was performed using *Phaser-MR* (Adams *et al.*, 2010) with lysozyme (PDB code 6irj; Lee *et al.*, 2019) as the search model. Model building and refinement were carried out using *Coot* (Emsley & Cowtan, 2004) and *Phenix.refinement* in *PHENIX* (Adams *et al.*, 2010), respectively. The geometries were analyzed using *MolProbity* (Williams *et al.*, 2018). The figures were generated by *PyMOL* (https://pymol.org/). The coordinates and structure factors have been deposited in the Protein Data Bank under the accession codes 6JXP (LCP-lysozyme) and 6JXQ (PAM-lysozyme). Diffraction images have been deposited in CXIDB under IDs 95 (LCP-lysozyme) and 96 (PAM-lysozyme).

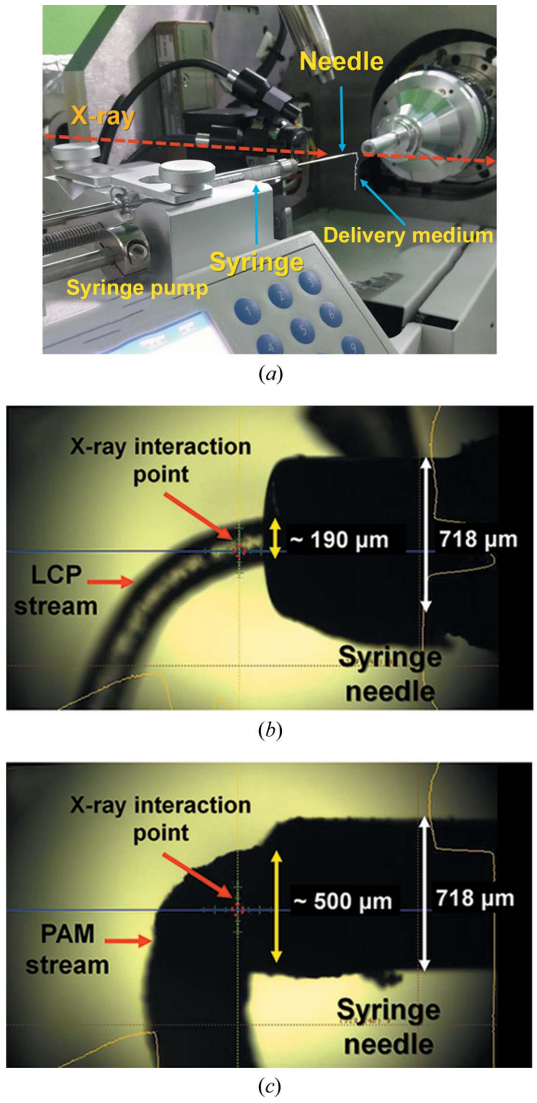

Figure 1
Syringe pump based sample delivery. (*a*) Experimental setup for sample delivery using a syringe and syringe pump. Snapshot of the injection stream of (*b*) LCP and (*c*) 10%(*w*/*v*) PAM delivery media.

3. Results and discussion

The syringe pump pushed the syringe plunger to extrude the sample from the syringe. In a preliminary study, we conducted a sample delivery test by setting the syringe and the needle directions to be vertical (Fig. 2). The delivery of non-viscous materials such as crystal suspension using a syringe pump is not suitable for the SX experiment because it forms a drop at the outlet of the syringe needle at a low flow rate [Fig. 2(*a*)]. Conversely, LCP and PAM as viscous sample delivery media provided very stable streams from the syringe needle with an inner diameter of 168 µm even at low flow rates of less than 100 nl min^{-1} using the syringe pump [Figs. 2(*b*) and 2(*c*)]. To demonstrate the capacity to collect SX data using the viscous delivery media, syringes and syringe pumps, we performed SMX experiments. In an ideal experimental setup, the syringe needle should be installed vertically in the sample delivery and the sample should flow downward. However, the syringe was

Table 1
Data collection and refinement statistics.

	LCP	PAM
Data collection		
Diffraction source	11C beamline, PLS-II	
Wavelength (Å)	0.94942	
Temperature (K)	298.15	
Detector	Pilatus 6M	
Crystal–detector distance (mm)	300	
Exposure time per image (s)	100 ms	
Space group	$P4_32_12$	
a, b, c (Å)	78.41, 78.41, 37.93	78.54, 78.54, 38.02
α, β, γ (°)	90, 90, 90	90, 90, 90
No. of collected images	40000	40000
No. of hits images	24258	24204
No. of indexed images	19411	21592
No. of unique reflections	17418 (1685)	12326 (1211)
Resolution range (Å)	78.7–1.56 (1.61–1.56)	79.3–1.76 (1.82–1.76)
Completeness (%)	99.93 (99.23)	100.0 (100.0)
Redundancy	318.4 (15.2)	770.4 (526.1)
$\langle I/\sigma(I)\rangle$	6.00 (1.26)	7.50 (1.60)
R_{split}†	9.87 (88.66)	7.40 (69.08)
CC	0.991 (0.436)	0.994 (0.380)
CC*	0.997 (0.779)	0.998 (0.742)
Overall B factor (Å^2)‡	23.56	36.99
Refinement		
Resolution range (Å)	55.53–1.56	55.44–1.76
Final R_{cryst}	16.75	17.42
Final R_{free}	20.03	20.19
R.m.s. deviations		
Bonds (Å)	0.010	0.010
Angles (°)	1.022	1.033
Average B factors (Å^2)		
Protein	31.64	46.43
Water	31.42	46.42
Ramachandran plot		
Most favored (%)	99.21	99.21
Allowed (%)	0.79	0.79

† Values for the outer shell are given in parentheses. ‡ Obtained from the Wilson plot.

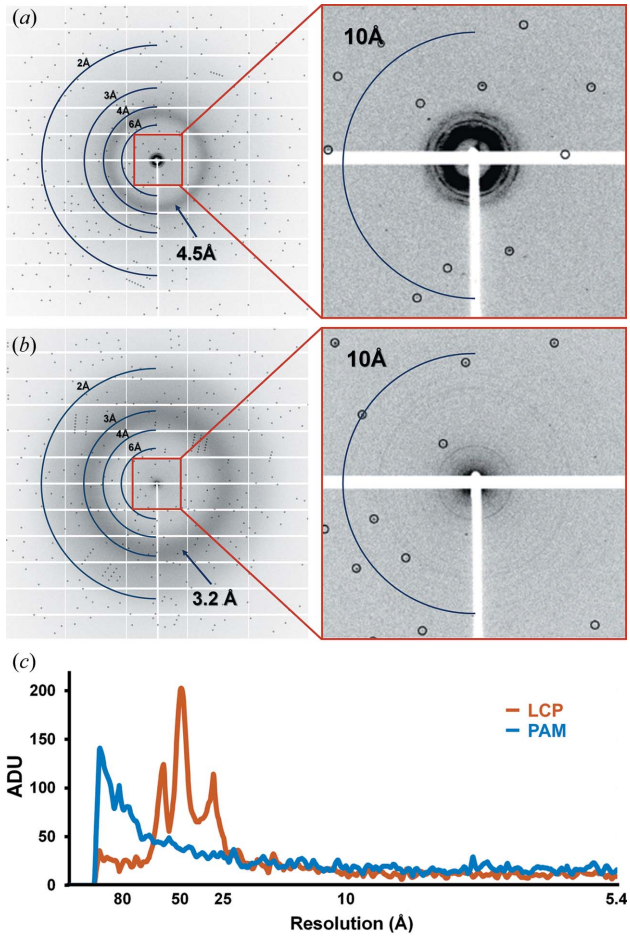

Figure 3
Room-temperature diffraction pattern of lysozyme delivered via (*a*) LCP and (*b*) PAM. (*c*) The two-dimensional profile of the scattering intensities of LCP (brown) and PAM (blue).

horizontally installed due to interference between the beamline equipment and the syringe pump. Viscous delivery materials that are extruded from syringe needles tend to curl without initially providing a stable stream. To address this issue, the syringe needle was first turned downward, and then the plunger was pushed manually to discharge the delivery material by about 10 mm. The discharged delivery material thus maintains a single stream without interruption due to viscosity and is thus directed downwards owing to gravity. In this state, if the delivery material is pushed at a low flow rate by using a syringe pump, it is delivered continuously and stably to the X-ray position along the previously discharged injection stream. Almost all samples passed the X-ray beam path [Figs. 1(*b*) and 1(*c*)]; however, the delivery medium was often found to be off the X-ray beam path. We consider that the vertical direction of the syringe needle will be helpful in maintaining a stable injection stream and the setup will be applied in further SX experiments. We collected 40 000 images of the lysozyme embedded in LCP and PAM using <2 mg lysozyme samples (Table 1). For the LCP delivery medium, the numbers of hit and indexed images were 24 258 (hit rate: 60.64%) and 19 411 (indexing rate: 80.01%), respectively. The diffraction images were processed up to 1.56 Å. The diffraction images using LCP included diffused background scattering at 4.5 Å [Fig. 3(*a*)], which was identical to that in the previous study (Weierstall *et al.*, 2014; Nam, 2019). For PAM delivery media, the numbers of hit and indexed images were 24 204 (hit rate: 60.51%) and 21 592 (indexing rate: 89.21%), respec-

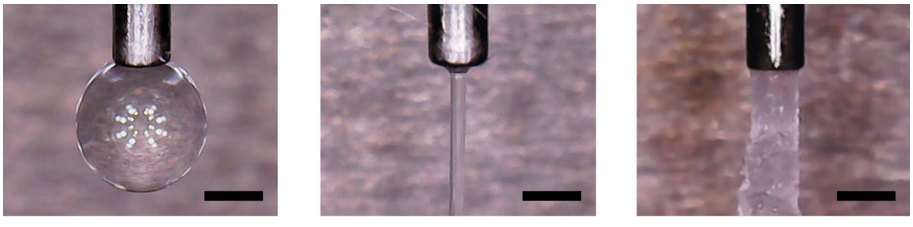

Figure 2
Snapshot of the sample delivery using the syringe and syringe pump. (*a*) Lysozyme crystal suspension in 100 m*M* sodium acetate, pH 4.6, 5% PEG 8000 and 10%(*w*/*v*) NaCl. (*b*) LCP delivery medium containing lysozyme crystals. (*c*) 10% (*w*/*v*) PAM delivery medium containing lysozyme crystals. Scale bar corresponds to 718 µm.

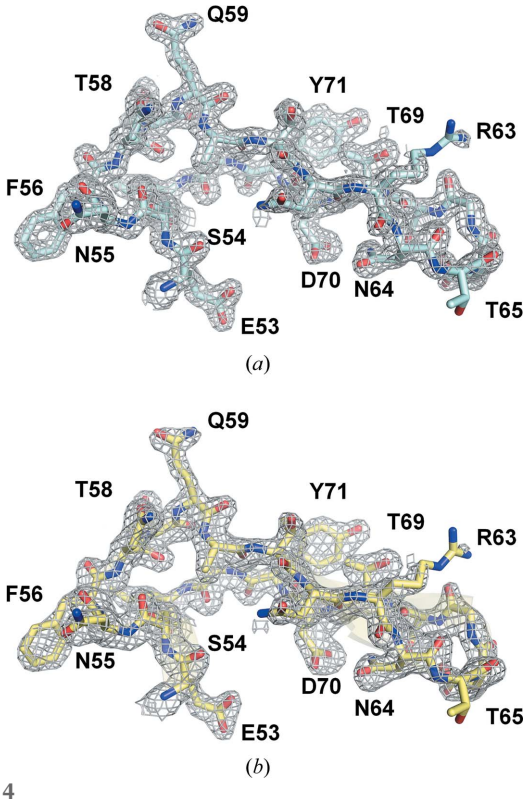

Figure 4
$2F_o - F_c$ electron density maps (gray mesh, 1.5σ) of room-temperature lysozyme structures delivered via (*a*) LCP and (*b*) PAM.

tively. The diffraction images were processed up to 1.76 Å. In the previous serial femtosecond crystallography experiment, the crystals embedded in PAM were delivered using the carrier matrix delivery injector, in which the pressure was applied to He gas from the outer capillary in the nozzle to guide the delivery medium towards the X-ray beam path (Park *et al.*, 2019). This He gas caused the dehydration of the PAM delivery sample and exhibited a scattering ring around 4.3 Å when the flow rate of the sample was less than 400 nl min^{-1} (Park *et al.*, 2019). Conversely, in this SMX experiment, the sample was delivered at a flow rate of 200 nl min^{-1} through the syringe needle, without guiding the injection stream using He gas. The image did not include the background scattering around 4.3 Å, which occurred when PAM was dehydrated, whereas scattering rings above 10 Å resolution were observed in the diffraction image [Fig. 3(*b*)] that were very weak and could be neglected in the data processing [Fig. 3(*c*)]. The final models of the lysozyme structures embedded in LCP and PAM were refined at 1.56 Å and 1.76 Å, respectively. Both electron density maps clearly exhibited the amino acids from Lys1 to Leu129 (Fig. 4). Specific radiation damage was not visible at the disulfide bonds in Cys24–Csy145, Cys82–Csy98 and Cys94–Csy112 (Fig. S1 of the supporting information).

4. Conclusions

In this study, we performed straightforward SX experiments using viscous media, a syringe and a syringe pump (this experimental setup is commercially available at a low cost). This method allows the beamline user to select the appropriate sample delivery medium for SX experiments in the laboratory. Due to the portability of the syringe pump, the same device that is used in the pre-experiment can be also used for data collection in the SX experiments. It not only enhances the reproducibility of the sample delivery during data collection but also enables efficient use of beam time. Meanwhile, we used a relatively large syringe needle with an inner diameter of 168 µm, which could be replaced by a syringe needle with an even smaller diameter to reduce sample consumption and background scattering. The smallest inner diameter of a commercially available syringe needle is about 51 µm. In this case, when using a sample that is several micrometres in size, experimental limitation in terms of sample consumption and background scattering may occur. Therefore, sample delivery using the aforementioned commercial syringe needle will be more useful when delivering crystal samples of several tens of micrometres in size. Our approach makes it easier for more crystallographers to access SX as well as more efficient use of beam time at synchrotrons and XFELs.

Acknowledgements

We thank the beamline staff at 11C beamline at Pohang Accelerator Laboratory for their assistance with data collection. The authors thank Global Science Experimental Data Hub Center (GSDC) at the Korea Institute of Science and Technology Information (KISTI) for computational support.

Funding information

The following funding is acknowledged: National Research Foundation of Korea (grant Nos. NRF-2017M3A9F6029736 to KHN and NRF-2016R1C1B1013601 to SYP); Korea University (grant No. KHN).

References

Adams, P. D., Afonine, P. V., Bunkóczi, G., Chen, V. B., Davis, I. W., Echols, N., Headd, J. J., Hung, L.-W., Kapral, G. J., Grosse-Kunstleve, R. W., McCoy, A. J., Moriarty, N. W., Oeffner, R., Read, R. J., Richardson, D. C., Richardson, J. S., Terwilliger, T. C. & Zwart, P. H. (2010). *Acta Cryst.* D**66**, 213–221.
Barty, A., Kirian, R. A., Maia, F. R. N. C., Hantke, M., Yoon, C. H., White, T. A. & Chapman, H. (2014). *J. Appl. Cryst.* **47**, 1118–1131.
Bohne, S., Heymann, M., Chapman, H. N., Trieu, H. K. & Bajt, S. (2019). *Rev. Sci. Instrum.* **90**, 035108.
Chapman, H. N., Caleman, C. & Timneanu, N. (2014). *Philos. Trans. R. Soc. London B Biol. Sci.* **369**, 20130313.
Emsley, P. & Cowtan, K. (2004). *Acta Cryst.* D**60**, 2126–2132.
Grünbein, M. L. & Nass Kovacs, G. (2019). *Acta Cryst.* D**75**, 178–191.
Kim, J., Kim, H.-Y., Park, J., Kim, S., Kim, S., Rah, S., Lim, J. & Nam, K. H. (2018). *J. Synchrotron Rad.* **25**, 289–292.
Lee, D., Baek, S., Park, J., Lee, K., Kim, J., Lee, S. J., Chung, W. K., Lee, J. R., Cho, Y. & Nam, K. H. (2019). *Sci. Rep.* **9**, 6971.
Nam, K. H. (2019). *Int. J. Mol. Sci.* **20**, E1094.
Nogly, P., James, D., Wang, D., White, T. A., Zatsepin, N., Shilova, A., Nelson, G., Liu, H., Johansson, L., Heymann, M., Jaeger, K., Metz, M., Wickstrand, C., Wu, W., Båth, P., Berntsen, P., Oberthuer, D., Panneels, V., Cherezov, V., Chapman, H., Schertler, G., Neutze, R.,

Spence, J., Moraes, I., Burghammer, M., Standfuss, J. & Weierstall, U. (2015). *IUCrJ*, **2**, 168–176.
Park, J., Park, S., Kim, J., Park, G., Cho, Y. & Nam, K. H. (2019). *Sci. Rep.* **9**, 2525.
Park, S. Y., Ha, S. C. & Kim, Y. G. (2017). *Biodesign*, **5**, 30–34.
Schulz, E. C., Mehrabi, P., Müller-Werkmeister, H. M., Tellkamp, F., Jha, A., Stuart, W., Persch, E., De Gasparo, R., Diederich, F., Pai, E. F. & Miller, R. J. D. (2018). *Nat. Methods*, **15**, 901–904.
Sugahara, M., Mizohata, E., Nango, E., Suzuki, M., Tanaka, T., Masuda, T., Tanaka, R., Shimamura, T., Tanaka, Y., Suno, C., Ihara, K., Pan, D., Kakinouchi, K., Sugiyama, S., Murata, M., Inoue, T., Tono, K., Song, C., Park, J., Kameshima, T., Hatsui, T., Joti, Y., Yabashi, M. & Iwata, S. (2015). *Nat. Methods*, **12**, 61–63.
Weierstall, U., James, D., Wang, C., White, T. A., Wang, D., Liu, W., Spence, J. C., Bruce Doak, R., Nelson, G., Fromme, P., Fromme, R., Grotjohann, I., Kupitz, C., Zatsepin, N. A., Liu, H., Basu, S., Wacker, D., Won Han, G., Katritch, V., Boutet, S., Messerschmidt, M., Williams, G. J., Koglin, J. E., Marvin Seibert, M., Klinker, M., Gati, C., Shoeman, R. L., Barty, A., Chapman, H. N., Kirian, R. A., Beyerlein, K. R., Stevens, R. C., Li, D., Shah, S. T., Howe, N., Caffrey, M. & Cherezov, V. (2014). *Nat. Commun.* **5**, 3309.
Weinert, T., Olieric, N., Cheng, R., Brünle, S., James, D., Ozerov, D., Gashi, D., Vera, L., Marsh, M., Jaeger, K., Dworkowski, F., Panepucci, E., Basu, S., Skopintsev, P., Doré, A. S., Geng, T., Cooke, R. M., Liang, M., Prota, A. E., Panneels, V., Nogly, P., Ermler, U., Schertler, G., Hennig, M., Steinmetz, M. O., Wang, M. & Standfuss, J. (2017). *Nat. Commun.* **8**, 542.
White, T. A., Mariani, V., Brehm, W., Yefanov, O., Barty, A., Beyerlein, K. R., Chervinskii, F., Galli, L., Gati, C., Nakane, T., Tolstikova, A., Yamashita, K., Yoon, C. H., Diederichs, K. & Chapman, H. N. (2016). *J. Appl. Cryst.* **49**, 680–689.
Williams, C. J., Headd, J. J., Moriarty, N. W., Prisant, M. G., Videau, L. L., Deis, L. N., Verma, V., Keedy, D. A., Hintze, B. J., Chen, V. B., Jain, S., Lewis, S. M., Arendall, W. B., Snoeyink, J., Adams, P. D., Lovell, S. C., Richardson, J. S. & Richardson, J. S. (2018). *Protein Sci.* **27**, 293–315.